Journal of Applied Mechanics and Technical Physics, Vol. 47, No. 6, pp. 825–835, 2006

LINEAR DRAINAGE IN A FRESH GROUNDWATER FRINGE ABOVE SALINE GROUNDWATER

V. N. Émikh

UDC 532.546.06

Possible flow variants as a function of the determining physical parameters are analyzed within the framework of the boundary-value problem of horizontal slit drainage in a fresh groundwater fringe above saline groundwater.

Key words: *freshwater fringe, linear drains, infiltration, mapping parameters, critical flow regime.*

Kapranov [1] constructed a solution of the Verigin problem of flow in a freshwater fringe to a system horizontal slit drains, which are further called linear drains, for their incomplete flooding. The unique solvability of the system of equations with respect to the mapping parameters related to the velocity hodograph was analytically established; in the calculations, a critical flow regime was found at the interface between fresh and saline groundwater. The present work reveals the physical content of the problem in the general formulation — with complete flooding of the drains.

1. Formulation and Solution of the Problem; Mapping Parameters. Stationary plane filtration in a fresh groundwater fringe above immovable saline water with uniform infiltration at rate ε is studied. The supply to the infiltration zone is compensated by outflow into equidistant linear drains of identical width located at the same depth. Because the flow is periodic, it is sufficient to study it within one half-period (Fig. 1).

In the case of complete flooding of the drains, the boundary-value problem describing the flow consists of finding its complex potential $\omega = \varphi + i\psi$ (φ is the filtration velocity potential and ψ is the stream function) normalized by the quantity $\varkappa L$ ($\varkappa$ is the ground permeability and L is half the distance between the centers of adjacent drains), which, in the filtration region, is an analytic function of the complex coordinate $z = x + iy$ normalized by L under the boundary conditions

$$CM\colon\quad x = 0,\quad \psi = 0; \qquad EN\colon\quad x = 0,\quad \psi = \varepsilon; \qquad AG\colon\quad x = 1,\quad \psi = \varepsilon;$$

$$MDN\colon\quad y = 0,\quad \varphi = 0; \qquad AC\colon\quad \varphi + y = 0,\quad \psi - \varepsilon x = 0; \tag{1}$$

$$EG\colon\quad \varphi - \rho y = \text{const},\quad \psi = \varepsilon \qquad (\rho = (\rho_2 - \rho_1)/\rho_1).$$

Here ρ_1 and ρ_2 are the densities of the fresh and saline water, respectively. The first condition on EG is a consequence of the assumptions that the saline water is motionless and that the pressure is continuous in passing through this segment. In Fig. 1, the depression curve AC is denoted by digit 1.

The problem is solved using the Polubarinova-Kochina method [2], which is based on using the analytical theory of linear differential equations. The method seeks to find the functions $\Omega = d\omega/d\zeta$ and $Z = dz/d\zeta$ determined in the half-plane $\operatorname{Im}\zeta \geqslant 0$ of the auxiliary complex variable $\zeta = \xi + i\eta$ (Fig. 2). The velocity hodograph $\bar{w} = w_x + iw_y$ (Fig. 3) is a circular polygon of the same form as that in the model of an infiltration fringe with tubular drainage [3]. The procedure of constructing the solution is also similar and eventually leads to the following relations:

Lavrent'ev Institute of Hydrodynamics, Siberian Division, Russian Academy of Sciences, Novosibirsk 630090; emikh@hydro.nsc.ru. Translated from Prikladnaya Mekhanika i Tekhnicheskaya Fizika, Vol. 47, No. 6, pp. 64–77, November–December, 2006. Original article submitted January 27, 2006.

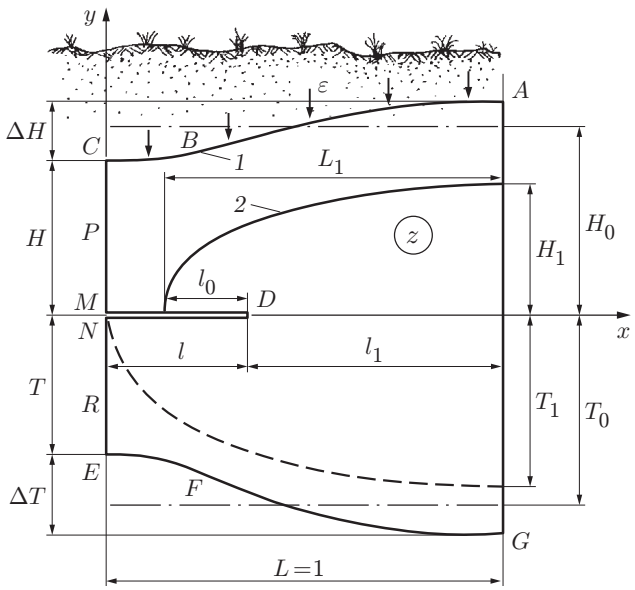

Fig. 1. Flow region in the freshwater fringe.

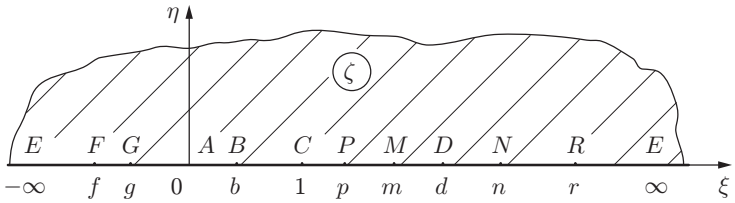

Fig. 2. Half-plane of the auxiliary complex variable.

$$\frac{d\omega}{d\zeta} = 2c_1F_1(\zeta)\lambda(\zeta), \qquad \frac{dz}{d\zeta} = -ic_1F_2(\zeta)\lambda(\zeta), \qquad c_1 > 0,$$

$$F_1(\zeta) = \sigma U - \frac{1}{U}, \qquad F_2(\zeta) = \alpha U + \frac{\beta}{U}, \qquad U = \exp\frac{W(\zeta)}{2}, \tag{2}$$

$$\lambda(\zeta) = \sqrt{\frac{(\zeta-p)(\zeta-r)}{(\zeta-g)\zeta(\zeta-1)(\zeta-m)(\zeta-n)}}.$$

For the function $\lambda(\zeta)$, we choose the branch which is positive for $\zeta > r$.

The function $W(\zeta)$ (Fig. 4) used to map the region of the complex filtration velocity $w = w_x - iw_y$ onto the half-plane $\operatorname{Im}\zeta \geqslant 0$ is given by the relations

$$W(\zeta) = \ln\frac{2i+\beta w}{2i\sigma - \alpha w} = ic_0\int\limits_0^\zeta \Phi(u)\,du \qquad (c_0 > 0),$$

$$\Phi(u) = \frac{(b-u)(u-f)}{(p-u)(r-u)}\,\Phi_0(u), \qquad \Phi_0(u) = \frac{1}{\sqrt{(u-g)u(1-u)}}, \tag{3}$$

$$\sigma = \frac{\sqrt{\varepsilon+\rho}+\sqrt{\varepsilon(1+\rho)}}{\sqrt{\varepsilon+\rho}-\sqrt{\varepsilon(1+\rho)}}, \qquad \alpha = \frac{\sigma-1}{\varepsilon} + \sigma + 1, \qquad \beta = \frac{\sigma-1}{\varepsilon} - \sigma - 1.$$

In Figs. 3 and 4, the circled letters C and E denote the corresponding points in the limiting cases, which will be considered in Sec. 2.

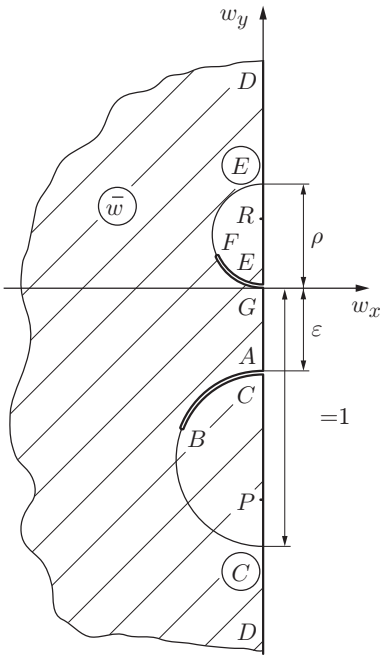

Fig. 3

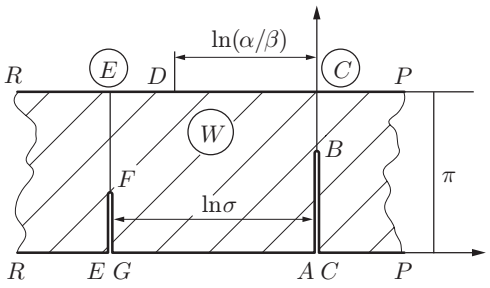

Fig. 4

Fig. 3. Filtration velocity hodograph.

Fig. 4. Intermediate region for mapping of the velocity hodograph onto the half-plane.

The function W contains the mapping parameters c_0, b, d, f, p, g, and r. As in [3], at the first stage, we solve the problem of finding the first five parameters with the two remaining parameters specified. The problem is solved as follows.

Five equations for the required parameters are derived using representation (3) and the known elements of the region W. During their transformation, the following auxiliary parameters are introduced:

$$k = \sqrt{-\frac{g}{1-g}}, \qquad s = \sqrt{\frac{1-g}{r-g}}, \qquad t = \sqrt{\frac{1-g}{p-g}}, \qquad \Theta = \sqrt{\frac{1-g}{d-g}}. \tag{4}$$

In the terms of (4), specifying the parameters g and r is equivalent to specifying the parameters k and s. The parameter t is expressed in terms of them using the following relation obtained by transformation of one of the five equations:

$$t = [s\Delta(\tau) + \tau\Delta(s)]/(1 - k^2 s^2 \tau^2),$$
$$\Delta(\chi) = \sqrt{(1-\chi^2)(1-k^2\chi^2)}, \qquad \tau = \operatorname{sn}\left[\ln\left(\sigma K'/\pi\right), k\right], \qquad K' = K(k'). \tag{5}$$

Here $K(k')$ is the complete elliptic integral of the first kind for the modulus $k' = \sqrt{1-k^2}$ and sn is the symbol of the elliptic Jacobi function [4].

The parameters c_0 and Θ are calculated from the other two transformed equations; the second of these parameters is linked, according to (4), to the parameter d:

$$c_0 k' = \frac{\pi}{2K'}\left[\Lambda_0(s,k') - \Lambda_0(t,k')\right] + \frac{\Delta(s)}{s} - \frac{\Delta(t)}{t}; \tag{6}$$

$$\frac{\pi}{2K'}\left[\Lambda_0(t,k') - \Lambda_0(s,k')\right][K - F(\Theta,k)] - K[Z(t,k) - Z(s,k)]$$
$$+ \frac{\Delta(s)}{s}\,\Pi\Big(\Theta, \frac{1}{s^2}, k\Big) - \frac{\Delta(t)}{t}\,\Pi\Big(\Theta, \frac{1}{t^2}, k\Big) = \ln\sqrt{\frac{\alpha}{\beta}}. \tag{7}$$

The above relations contain incomplete elliptic integrals of the first kind $F(\Theta, k)$ and third kind $\Pi(\Theta, n, k)$ and the standardized lambda-function $\Lambda_0(\delta, k')$ and zeta-function $Z(\delta, k)$ [4].

The parameters b and f are found as roots of the quadratic equation

$$\Gamma(\gamma) = \gamma^2 - [p + r - a(R - P)]\gamma + pr - a(pR - rP) = 0,$$
$$a = c_0^{-1}, \qquad P = \Phi_0^{-1}(p), \qquad R = \Phi_0^{-1}(r). \tag{8}$$

The unique solvability of system (5)–(8) is established analytically for the following constraints on the parameters k and s:

$$k_0 \leqslant k < 1, \qquad 0 \leqslant s \leqslant s_0. \tag{9}$$

Here k_0 is a root of the equation

$$K(k_0)/K(k_0') = \ln \sigma/\pi \qquad (k_0' = \sqrt{1 - k_0^2}). \tag{10}$$

The quantity s_0 is defined by the equality

$$s_0 = \sqrt{(1 - \tau^2)/(1 - k^2\tau^2)}. \tag{11}$$

The coefficient c_1 in Eqs. (2) plays the role of a scaling factor and can be eliminated from the computational relations by using the relation that fixes the quantity L (by which the coordinates z are normalized) and follows from relations (2) and (3) after their transformation as applied to the segment EG (see Figs. 1, 2, and 4):

$$c_1 \frac{\alpha + \beta\sigma}{\sqrt{\sigma}} \int\limits_{-\infty}^{g} \cos \frac{W_0(\zeta)}{2} \, |\lambda(\zeta)| \, d\zeta = 1,$$
$$W_0(\zeta) = c_0 \int\limits_{-\infty}^{\zeta} \frac{(b - u)(f - u) \, du}{(p - u)(r - u)\sqrt{(g - u)(-u)(1 - u)}}. \tag{12}$$

Specifying the length l of the segments MD and ND and using (2), we obtain the following system of equations for the parameters m and n:

$$c_1 \int\limits_{m}^{d} \Big(\alpha U - \frac{\beta}{U}\Big) |\lambda(\zeta)| \, d\zeta = l, \qquad c_1 \int\limits_{d}^{n} \Big(\frac{\beta}{U} - \alpha U\Big) |\lambda(\zeta)| \, d\zeta = l,$$
$$U = \exp \frac{W_1(\zeta)}{2}, \qquad W_1(\zeta) = c_0 \int\limits_{1}^{\zeta} \frac{(u - b)(u - f) \, du}{(p - u)(r - u)\sqrt{(u - g)u(u - 1)}}. \tag{13}$$

As in other problems of this kind, in deriving one of the two equations for the parameters k and s, we specify the depth T_0 of the initial saline water surface, which is indicated in Fig. 1 by a dash-and-dotted straight line. Under the assumption that the volume of saline water remains unchanged during the formation of the fringe, the value of T_0 is equal to the average ordinate of the points of the interface EG. Proceeding from this, we obtain the equation

$$T + \frac{c_1^2(\beta^2\sigma^2 - \alpha^2)}{\sigma} \int\limits_{\infty}^{g} \Big(\int\limits_{\infty}^{\zeta} \sin \frac{W_0(u)}{2} \, |\lambda(u)| \, du \Big) \cos \frac{W_0(\zeta)}{2} \, |\lambda(\zeta)| \, d\zeta = T_0. \tag{14}$$

In using it, we need to preliminarily calculate the quantity of T, which is expressed from relations (2) and (3) after their transformation as applied to the segment NE.

Among the determining physical parameters is the pressure head h on the drain; this quantity is linked to the normalized filtration velocity potential φ by the relation

$$\varphi = -h, \qquad h = p/(\rho_1 g) + y. \tag{15}$$

Here p is the flow pressure.

The corresponding equation is obtained by deriving the expression for the potential φ at the point M located on the drain. This expression depends on the position of the point P (see Figs. 3 and 4), at which

$$W = \infty, \qquad w_x = 0, \qquad w_y = -2\sigma/\alpha > -1. \tag{16}$$

According to (15), the following relation holds on the segment CM:

$$\frac{dp}{dy} = -\rho_1 g(w_y + 1).$$

This relation and the inequality in (16) imply that $(dp/dy)_P < 0$: the point P is on the segment of increasing pressure for motion downward from the point C and, by virtue of this, it can be located on the drain only when the pressure at the drain exceeds atmospheric pressure; otherwise, the point P belongs to the segment CM and divides it into two segments. In the latter case, the equation based on specifying the quantity h_M is obtained, by using relations (2), in the form

$$H - 2c_1\Big[\int\limits_1^p \Big(\sigma U - \frac{1}{U}\Big)|\lambda(u)|\,du - \int\limits_p^m \Big(\sigma U + \frac{1}{U}\Big)|\lambda(u)|\,du\Big] = h_M. \tag{17}$$

The function $U(\zeta)$ is defined in (13).

In the case $P \in MN$, the quantity h_M is given by the equality

$$H - 2c_1 \int\limits_1^m \Big(\sigma U - \frac{1}{U}\Big)|\lambda(u)|\,du = h_M. \tag{18}$$

The ordinate H of the point C contained in the last equations should be calculated previously using representation (2) for $z(\zeta)$.

The programmed algorithm for determining the mapping parameters for the specified physical parameters ε, ρ, h_M, l, and $L = 1$ eventually reduces to finding the parameter k from Eq. (14), whose left side is treated as a composite function of the indicated parameter. For each of its values fixed during this iterative procedure, one of Eqs. (17) or (18) for the parameter s is solved numerically; in both these cycles, the required parameters are subject to constraints (9). Next, in the internal part of the algorithm, the parameters c_0, b, d, f, and p are determined from Eqs. (5)–(8), and the coefficient c_1 and the mapping parameters m and n are determined from Eqs. (12) and (13). The unique solvability of Eqs. (13), (14), and (17) [or (18)] is ensured by the numerically established monotonicity of the functions included in these equations.

2. Limiting and Particular Cases. As in the problem of a fringe with tubular drainage, the problem of physical premises for the formation of flow to flooded linear drains is related primarily to constraints (9). Because in both filtration models, the velocity hodograph is the same, the previous analysis (see [3, Sec. 3]) of the limiting drainage regimes involving the indicated constraints is completely extended to the flow being studied. The main results of this analysis are as follows.

Case $s = s_0$. In this case, $p = b = 1$, i.e., the point B of inflection of the depression curve and the point P of the segment CM coincide with the point C, which becomes the apex of the depression curve. The half-disc $|\bar w + i(1+\varepsilon)/2| < (1-\varepsilon)/2$, $\operatorname{Re}\bar w \leqslant 0$ falls out of the filtration velocity hodograph, and the half-band $\operatorname{Re} W > 0$, $0 \leqslant \operatorname{Im} W \leqslant \pi$ falls out of the region W (see Figs. 3 and 4). On the segment CM, we have $dp/dy = -\rho_1 g(w_y+1) \leqslant 0$, where the equality satisfied only at the point C, and at the remaining points, the pressure is below atmospheric pressure and its further arbitrarily small decrease should lead to air penetration into the drain. This implies that in the case considered, the drainage rate is maximum admissible and should be established previously and that the critical flow regime occurs in the case of drainage pumping [5]. In practice, vacuum tubular drainage is used in land reclamation [6], but for linear drains, this regime is not characteristic and is rather of theoretical interest.

Case $s = 0$. In this case, $r = -f = \infty$: the points R and F coincide with the point E, which becomes the apex of the interface, and at this point, $\bar w = i\rho$. As a result, the half-disk $|\bar w - i\rho/2| < \rho/2$, $\operatorname{Re}\bar w \leqslant 0$ falls out of the hodograph, and the half-band $\operatorname{Re} W < \ln\sigma$, $0 \leqslant \operatorname{Im} W \leqslant \pi$ falls out of the region W (see Figs. 3 and 4). On the segment EN, where also $\bar w = iw_y$, we have $w_y \geqslant \rho$, $dp/dy = -\rho_1 g(w_y+1) \leqslant -\rho_2 g$. In this case, the equality characterizing the hydrostatic equilibrium in the saline water zone is satisfied only at the point E. On the remaining part of the segment EN, the hydrodynamic-pressure gradient exceeds the hydrostatic-equilibrium gradient in the f saline water zone, and further pressure decline should entrain the water in the flow.

The indicated regime occurs at the limit of destabilization of the interface between fresh and saline water and, hence, it also should be calculated previously. The question is what of the two critical situations occurs for particular values of the determining physical parameters.

Case $s_0 = 0$. This limiting case, first noted in [7] as the *a double critical regime*, combines the *simple critical regimes* described above and, at the same time, separates them; for this reason, the double critical regime is to be first calculated. In the case considered, both half-disks fall out of the hodograph, and the region W becomes a rectangle which is mapped onto the half-plane $\operatorname{Im}\zeta \geqslant 0$ by the relation

$$W(\zeta) = i\,\frac{\pi}{K_0'}\,F\Big(\sqrt{\frac{\zeta}{k_0^2 + k_0'^2\zeta^2}}, k_0'\Big), \tag{19}$$

where $K_0' = K(k_0')$. The moduli k_0 and k_0' are determined from (10).

From Eq. (7), we obtain

$$\Theta = \operatorname{sn}\left((K_0'/\pi)\ln(\beta\sigma/\alpha), k_0\right)$$

and then from the last equality in (4), we find the parameter d. Equations (12) and (13) for the parameters c_1, m, and n and the remaining computational formulas are also considerably simplified. In this case, $\lambda(\zeta) = 1/\sqrt{\zeta(\zeta - g)}$, and the function $W(\zeta)$ is calculated according to (19).

From the previous analysis of the limiting case $s = s_0$, it follows that one of the premises for the occurrence of the double critical regime is drainage pumping.

Let us consider filtration in the freshwater fringe to the partially flooded drains. In relation to the model considered in Sec. 1, this case is a particular one: the depression curve (curve 2 in Fig. 1) intersects the drain orthogonally, and the velocity hodograph has the same form as that in the limiting case $s = s_0$, but the flow studied occurs in the *normal regime*. Appropriate changes should be made in relations (2) and (3), which represent the solution of the problem: in this case, the function $\lambda(\zeta)$ does not contain the factors $\zeta - p$ and $\zeta - m$, and the function $\Phi(u)$ the factors $b - u$ and $p - u$.

The determination of the mapping parameters using the algorithm described above eventually reduces to finding the parameter k from the relation to which Eq. (14) is transformed. For each value of this parameter fixed during the solution of the equation in the interval $(k_0, 1)$, the parameter $s = s_0$ is calculated using relations (11), (5), and (3). According to (5), we have $t = 1$, and Eqs. (6) and (7) are transformed as follows:

$$c_0 k' = \frac{\Delta(s)}{s} - \frac{\pi}{2K'}\,[1 - \Lambda_0(s, k')],$$

$$\int\limits_{\Theta}^{1} \frac{(\Delta(s)/s)u^2 - c_0 k'(u^2 - s^2)}{\Delta(u)(u^2 - s^2)}\,du = \ln\sqrt{\frac{\alpha}{\beta}}.$$

In this case, $p = 1$; from (8), we obtain $f = r - aR$ [the parameter r is expressed in terms of s on the basis of the second equality in (4)].

The coefficient c_1 and the parameter n are found from the transformed equation (12) and the second equation in (13). For $m = 1$, the first equation in (13) is transformed to the equality, from which the width l_0 of the flooded segment of the drains is determined.

The only critical regime possible in the flow considered is due to the presence of the interface, whose destabilization is promoted by both enhancement of infiltration and a decrease in the drain width. In [1], this regime was detected for the first time as a manifestation of the second of these factors: the extension of the zone of action of infiltration water on saline water can lead to expulsion of the latter to the drains. In this case, the velocity hodograph, the region of the function W, and all their associated relations are the same as those in the double critical flow regime to the completely flooded drain, and the representations for the functions $\omega(\zeta)$ and $z(\zeta)$ and their related formulas do not contain the coefficient $\zeta - m$.

In the determination of the saline water depth, a key role is played by the problem of a drained freshwater lens resulting from uniform infiltration, considered by Polubarinova-Kochina [8]. This is the first model for the two-dimensional filtration of liquids of different densities that, in the problem studied, describes the critical regime in which the apex point E of the interface (dashed curve in Fig. 1) coincides with the point N when entering the drain

and the zone breaks up into a chain of lenses. Both of the free boundaries of the lenses are arcs of ellipses whose common focal points are located at the terminal points of the drains; in terms of the dimensionless (normalized by L) geometrical quantities, their semiaxes are defined by the equalities (see Fig. 1)

$$1 = l_1\sqrt{\frac{(1+\rho)(\varepsilon+\rho)}{\rho(1+\varepsilon+\rho)}}, \qquad T_1 = l_1\sqrt{\frac{\varepsilon}{\rho(1+\varepsilon+\rho)}}, \tag{20}$$

$$L_1 = l_1\sqrt{\frac{1+\rho}{(1-\varepsilon)(1+\varepsilon+\rho)}}, \qquad H_1 = l_1\sqrt{\frac{\varepsilon(\varepsilon+\rho)}{(1-\varepsilon)(1+\varepsilon+\rho)}} \qquad (l_1 = 1-l).$$

The situation considered arises for $\varepsilon = \varepsilon_0$ and $T_0 = T_{00}$; the parameter ε_0 is determined from the first relation in (20), and the quantity T_{00} is calculated on the basis of the equalities obtained using the well-known relations for the geometrical parameters of the ellipse:

$$T_{00} = (\pi/4)T_1, \qquad T_1^2 = 1 - l_1^2. \tag{21}$$

The same value of the quantity T_{00} can be obtained from the second equality in (20) for $\varepsilon = \varepsilon_0$.

3. Hydrodynamic Analysis of the Problem. The theoretical investigation performed above, together with numerical calculations, reveal the diversity of the hydrodynamic content of the formulated boundary-value problem. The only rigorous foundation for such an analysis is the direct formulation, in which the implementation conditions are established within the framework of the problem of the flow modeled and the dependence of flow characteristics on the determining physical factors is studied; among the latter, the infiltration rate is the most dynamic and, in some cases, controllable parameter.

In particular cases, the computational algorithm depends on whether the drains are partially or completely flooded, and to maintain the normal drainage regime it is necessary that the specified value of the parameter ε be matched to the value of T_0. In this connection, for chosen values of l and ρ, one needs to determine the infiltration rate and the initial depth of saline water in the situation where the depression curve reaches the drain at the point M and the critical regime occurs at the interface. In this case, which will be called the *boundary-critical* case, the calculations are performed for the model of partial flooding of the drains for $l_0 = l$.

Because the interface should not reach the drains, we return to the model of Polubarinova-Kochina mentioned in Sec. 2. From the first and third equalities in (20), we conclude that in this limiting model for $L_1 = 1$, the following relations hold:

$$\varepsilon = \varepsilon_0^* = 1 - \rho, \qquad l = l_* = 1 - \sqrt{2\rho/(1+\rho)}. \tag{22}$$

For real values of the parameters ε and ρ, which are hundredth and thousandth of unity, we have $\varepsilon < \varepsilon_0^*$ and $L_1 < 1$; this implies that, as a rule, in the critical regime, the interface reaches the drain which is partially flooded. Complete flooding occurs for drains of small width; in these cases, the interface in the boundary-critical regime is below the drains. For this flow, the quantities $\varepsilon = \varepsilon_*$ and $T_0 = T_0^{**}$ are calculated.

In the case $\varepsilon < \varepsilon_*$, the drain is partially flooded with the depression curve reaching it if the pressure on the drain is equal to atmospheric pressure; otherwise, the drain is completely flooded. The saline water depth should satisfy the inequality $T_0 > T_0^*$, in which the quantity T_0^* is previously determined for the specified value of ε in the critical regime associated with the interface. According to calculations of $T_0^* \in (0,\ T_0^{**})$, this extension of the range of admissible values of the initial saline water depth is a response to a decrease in the infiltration rate. We note that if the quantity $T_0 = T_0^*$ is included in the number of determining parameters, the value of ε for which the quantity T_0^* was calculated should be treated as the maximum admissible infiltration rate.

The case $\varepsilon > \varepsilon_*$ requires a preliminary analysis because with the recession of saline water, their supporting effect on the filtration flow weakens. In this case, one should expect a decline of the depression curve. In this connection, the question arises: Can the depression curve reach the drain when the infiltration is at least slightly higher than ε_*? A sufficiently unambiguous answer to this question is provided by numerical calculations with double accuracy for a controlled relative error not higher than 10^{-4}.

Let us consider flow for $l = 0.1$ and $\rho = 0.01$. In this case, for the boundary-critical regime, we have $\varepsilon_* = 0.3388$, $\Delta H = 0.4240$, $T_0^{**} = 1.5410$, $\Delta T = 0.6294$. The large value of the parameter ε is due to the fact that the value of l is also chosen to be considerable from a practical point of view in order to reflect the specificity of

linear drainage. We note that for 0.001, 0.01, and 0.5, we obtained $\varepsilon_* = 0.00473$, 0.0454, and 0.8588, respectively. As regards the parameter ρ, it has little effect on the value of ε_*; for example, for $l = 0.1$ and $\rho = 0.0001$ and 0.1, we obtained $\varepsilon_* = 0.3388$ and 0.3382, respectively. The value of $\rho = 0.01$ adopted in the calculations corresponds to a mineral content of saline water equal to approximately 13 g/liter for NaCl [9].

For an infiltration $\varepsilon = 0.34$, which is slightly higher than its threshold value ε_*, and for $h_M = 0$, i.e., for the preservation of atmospheric pressure on the drain, in the critical regime at the interface, we have $H = 0.02243$, $\Delta H = 0.4031$, $T_0^* = 1.5417$, and $\Delta T = 0.6294$. Next, for the same infiltration and $T_0 = 2.0$, 2.5, and 3.0, the calculation yields $\Delta T = 0.0914$, 0.0188, and 0.0039, respectively, which implies that the interface flattens out with increasing depth. Meanwhile, the depression curve practically does not react to the recession of saline water: for all indicated values of T_0, with accuracy up to four significant figures, we obtained $H = 0.02237$ and $\Delta H = 0.4032$. A similar situation occurs for other small values of ρ, which allows the calculations for $\varepsilon > \varepsilon_*$ and $T_0 > T_0^*$ to be performed within the framework of the model of complete flooding of the drains. Among the parameters determining the flow in this case, one needs to specify the pressure on the drain, to which Eq. (17) or Eq. (18) is related. If the pressure on the flooded drain is equal to or else higher than atmospheric pressure, the only possible critical flow regime for the specified infiltration $\varepsilon > \varepsilon_*$ is due to the presence of the interface. The calculation of this flow establishes the minimum admissible depth T_0^* of saline water.

Starting from the boundary-critical regime, we examine the effect of increasing the infiltration rate on the freshwater fringe for $h_M = 0$. A natural result of this is a rise of the depression curve, which is accompanied by its flattening due to gradual recession from the drain; in particular, for $\varepsilon = 0.4$, 0.6, 0.8, and 0.9, the calculation gives the following values, respectively: $H = 0.2019$, 0.8213, 2.3605, and 5.3146 and $\Delta H = 0.3045$, 0.1180, 0.00298, and $6 \cdot 10^{-7}$. This factor has a less significant effect on the position of the interface in the critical regime and almost no effect on the deformation of the interface: for $\varepsilon = 0.4$ and 0.9, we obtained $T_0^* = 1.5757$ and 1.8059; $\Delta T = 0.6301$ and 0.6333, respectively.

An increase in the pressure head on the drain has a similar effect on the shape and position of the depression curve, whereas the effect of this factor on the average depth of the interface and its deformation is even smaller than that of infiltration. Thus, for $\varepsilon = 0.4$ and $h_M = 3$, we have $T_0^* = 1.5499$ and $\Delta T = 0.6292$. A certain reduction in the critical depth of saline water is a manifestation of the damping effect of an increase in the thickness of the freshwater fringe with increasing pressure head on the drain.

As noted in Sec. 2, vacuum linear drainage is not typical of practice; nevertheless, for completeness of the analysis, we consider this case. In particular versions with specified values of the quantities l, ρ, and $\varepsilon > \varepsilon_*$, one first needs to calculate the double critical regime, which determines the minimum admissible values of the pressure head $h_M^{**} < 0$ on the drain and the initial depth T_0^* of saline water. For $l = 0.1$, $\rho = 0.01$, and $\varepsilon = 0.34$, 0.4, 0.6, 0.8, and 0.9, we obtain $h_M^{**} = -0.00017$, -0.0176, -0.1284, -0.3045, and -0.4231, and $T_0^* = 1.5418$, 1.5810, 1.6878, 1.7706, and 1.8064, respectively. From a comparison of these values of T_0^* with its values for $\varepsilon = 0.4$ and 0.9 and $h_M = 0$ given above, it follows that drainage pumping by itself only leads to an insignificant increase in the critical depth of saline water. The pressure decline on the drain has little effect on the deformation of the interface: for $\varepsilon \in (0.4, 0.9)$ in the double critical regime, the value of ΔT varies in the same range as for $h_M = 0$: $\Delta T \in (0.6302, 0.6333)$.

The above-mentioned extremely weak effect of the density of saline water on the infiltration rate ε_* in the boundary-critical regime is also manifested in relation to the value of h_M^{**}; in particular, for $l = 0.1$, $\varepsilon = 0.6$, and $\rho = 0.0001$ and 0.1, we obtained $h_M^{**} = -0.1284$ and -0.1288, respectively. The values of H and ΔH also change insignificantly. As regards the interface, its deformation and, particularly, position depend significantly on the parameter ρ: for the above-mentioned values of the parameter in the double critical regime, we obtain $T_0^* = 3.1513$ and 0.9750 and $\Delta T = 0.6366$ and 0.5936, respectively.

For $T_0 > T_0^*$, the flow regime at the interface is normal, and the minimum admissible pressure head on the drain h_M^* is determined by calculating the simple critical regime on the depression curve. However, with increasing T_0, the value of h_M^{**} calculated for the double critical regime remains unchanged up to the fourth significant figure, which eliminates the need for special calculations to find the value of h_M^*.

For $h_M > h_M^{**}$, where the depression curve is formed in the normal regime, the only constraint is due to the quantity T_0. Its minimum admissible value is established by calculating the flow in the simple critical regime at the interface, although in this situation, too, as T_0^* one can use its value obtained for the double critical regime. For example, for $\varepsilon = 0.6$ and $\rho = 0.01$ in the wide range of the pressure head h_M on the drain increasing from the

minimum value of -0.1284 in the double critical regime to unity, the value of T_0 in the corresponding simple critical regimes at the interface decreases from 1.6878 to 1.6777.

Let us study the flow characteristics for $\varepsilon < \varepsilon_*$, assuming as before that $l = 0.1$ and $\rho = 0.01$. As noted above, the drain is completely flooded in this case, too, if $h_M > 0$. Thus, for an infiltration $\varepsilon = 0.1$, which is significantly smaller than the value of $\varepsilon = 0.3388$ for the boundary-critical regime, and for $h_M = 0$ in the critical regime at the interface, we have $l_0 = 0.0124$, i.e., only a small part of the drain is flooded. For $h_M = 0.01$, the minimum thickness of the water layer above the drain is $H = 0.0111$. With further increase in the pressure head, just as in the case $\varepsilon > \varepsilon_*$, the depression curve rises and flattens out and the average depth of the interface in the critical flow regime decreases slightly with retention of its deformation.

The regularities detected for $\varepsilon > \varepsilon_*$ are true for the chosen parameters l, ε, and ρ and $h_M = 0$. The depression curve is little affected by the position of the lower boundary of the flow, and the latter flattens out with increasing depth: the value of ΔT decreases from $\Delta T = 0.6190$ to $\Delta T = 3 \cdot 10^{-6}$ as T_0 increases from the minimum value of $T_0 = 1.2597$ in the critical regime to $T_0 = 5$. As regards the density of saline water, for its variation and a fixed value of T_0, the values of l_0 and H_1 are retained up to the seventh or eighth significant figure.

For the critical regime at the interface, the parameter ρ also has an insignificant effect on the nature of the depression curve: as this parameter increases in the range $\rho \in (0.0001, 0.1)$ and T_0^* decreases simultaneously from $T_0^* = 2.7167$ to $T_0^* = 0.5956$, the quantities l_0 and H_1 increase in the intervals $l_0 \in (0.0124, 0.0126)$ and $H_1 \in (0.1384, 0.1428)$. However, even with that insignificant variation of these quantities, one observes a supporting effect on the flow from the interface during its rise. This effect is most pronounced for large values of the parameter ρ. In particular, for $\rho = 10^6$, the values of $l_0 = 0.0124$ and $H_1 = 0.1384$, remaining almost unchanged at $T_0 \geqslant 1.5$, increase to $l_0 = 0.0253$ and $H_1 = 0.2219$ at $T_0 = 0.05$ as the interface rises. In this case, the quantity ΔT reaches the maximum value $\Delta T = 2 \cdot 10^{-7}$, and, hence, in the case considered, the lower boundary becomes a horizontal confining layer. For the same values of the parameters ρ and l as in the previous example and $\varepsilon = 0.34$, the pressure head from the lower boundary of the flow is manifested at $T_0 < 1.5$ in rise and flattening of the depression curve. The average ordinate H_0 of its points increases from $H_0 = 0.3361$ for large values of T_0 to $H_0 = 0.4263$ for $T_0 = 0.1250$, and the quantities H and ΔH vary from values of $H = 0.0224$ and $\Delta H = 0.4032$, respectively, to values of $H = 0.1825$ and $\Delta H = 0.3477$.

For $T_0 < T_{00}$, the critical flow regime is beyond the scope of the boundary-value problem being studied; therefore, the constraint on the infiltration rate can be established only approximately. For this, we orient ourselves to the corresponding value of $\varepsilon = \varepsilon_{00} < \varepsilon_0$ determined by the second equality in (20), in which, in view of (21), it is necessary to set $T_1 = (4/\pi)T_0$. The right side of the first equality in (20), from which the value of ε_0 was calculated for $T_0 = T_{00}$, now determines the quantity $L_* < 1$, which, together with the quantities T_0 and ε_{00}, are the parameters of the flow with the interface entering the drain [8]. This limiting situation fits the basic flow pattern for $L = L_*$ with retention of the distance $2l_1$ between the terminal points of adjacent drains (see Fig. 1). For $L > L_*$, the normal filtration regime is retained not only for an infiltration $\varepsilon = \varepsilon_{00}$ but also in the case of its excess. The degree of this excess, as noted above, can be determined approximately by calculations.

For $l = 0.1$ and $\rho = 0.1$ for the limiting regime with entry into the drain, calculations by formulas (20) and (21) gave values of $T_{00} = 0.3423$, $\varepsilon_0 = 2.3747 \cdot 10^{-3}$, and $l_0 = 1.3098 \cdot 10^{-3}$. For a fixed value of $T_0 = 0.2$, we have $L_* = 0.9353$, $\varepsilon_{00} = 8.092 \cdot 10^{-4}$, and $l_0 = 3.897 \cdot 10^{-4}$. The last two parameters can be compared with the parameters ε_0 and l_0 given above if we set $L = L_*$. For an initial value of $L = 1$, the range of admissible values of the parameter ε is extended, and for $\varepsilon = \varepsilon_{00}$, the flow occurs in the normal regime; in this case, $T = 0.0424$ and $l_0 = 2.257 \cdot 10^{-4}$. As the infiltration increases, the interface approaches the drain, and for $\varepsilon = 1.1\varepsilon_{00} = 8.901 \cdot 10^{-4}$ (at the limit of the capabilities of the computational algorithm), we have $T = 0.0108$ and $l_0 = 3.597 \cdot 10^{-4}$. Obviously, the latter value of ε is close to the maximum admissible value. For $L = 1.2$, the flow characteristics were calculated for $\varepsilon = 1.25\varepsilon_{00} = 1.012 \cdot 10^{-3}$, in particular, the calculations gave values of $T = 0.0497$ and $l_0 = 2.794 \cdot 10^{-4}$. The indicated overloads in the calculations are due to the fact that in such cases, some mapping parameters take nearly limiting values. For example, in the latter version, $d = 1.000083$, $g = -0.00812$, and $n = 2{,}789{,}388$. In this case, $r = 38.365$: the point R is located on the segment DN, i.e., on the lower surface of the drain (see Figs. 1 and 2).

Boundary conditions (1), which correspond to the flow pattern for complete flooding of the drains, include the equality $x = 0$, which is common for the segments CM and EN. This equality expresses that they belong to the line of symmetry of the flow and is used in Eqs. (13). This requirement, dictated by the original physical

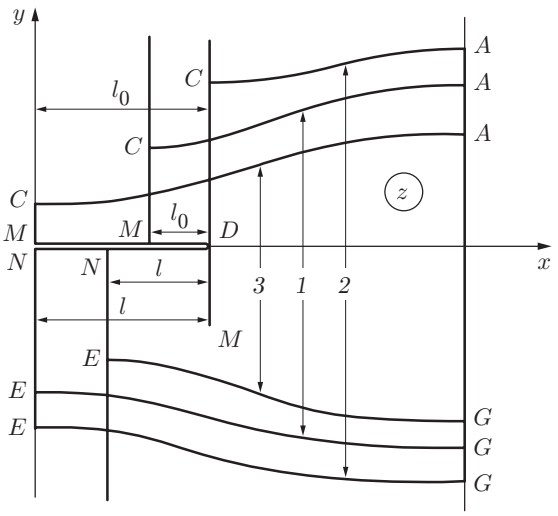

Fig. 5. Modified flow patterns.

formulation, does not affect the geometry of the flow region in the neighborhood of singular points and, eventually, the velocity hodograph. Hence, we can depart from the condition $|MD| = |ND|$ and consider some modifications of the original physical formulation of the boundary-value problem formulated in Sec. 1, retaining the solution representation (2) and the computational algorithm described above and taking into account that the right side of the first equation in (13) now contains the quantity l_0, which differs from the quantity l. For $l_0 < l$, the flow pattern can be treated as inflow to a basin of width $2(l - l_0)$ with impermeable sidewalls and drainage under the basin that protrudes a distance l_0 beyond its walls; the free boundaries of this flow are denoted by digit 1 in Fig. 5. Digit 2 denotes the boundaries of the flow to the basin, whose walls are embedded in ground. In this case, the singular point M passes onto the segment ND, and, hence, $d < m < n$, and the quantities l and l_0 in Eqs. (13) denote the width of the basin and the depth of the shield, respectively; in the second equation, the low limit of integration is the parameter m. For $l_0 > l$, the flow denoted by digit 3 in Fig. 5 occurs. It can also be interpreted physically by assuming that under the middle part of the drain there is an impermeable inclusion of width $2(l_0 - l)$ with vertical walls that and water on this segment enters the drain only from above.

For input parameters $\rho = 0.01$, $\varepsilon = 0.1$, $l = 0.1$, and $T_0 = 1.5$, the value of $l_0 = 0.0124$ in the initial flow pattern determines the abscissa of the point of entry of the depression curve into the drain. We use this point as the control one. The first of the patterns listed above occurs if the vertical wall is located to the right of the indicated point. As the shield is displaced to the right to the terminal point of the drain and is then deepened with transition to the second modified pattern, the supporting effect of the shield on the flow is enhanced, resulting in a rise and flattening of the depression curve: the quantities H and ΔH, which have values $H = 0$ and $\Delta H = 0.1223$ when the shield enters the drain at the control point, take values $H = 0.4447$ and $\Delta H = 0.0073$ for $l_0 = 30$ in the second pattern. At the same time, the interface is significantly deformed: for the indicated variation of the position of the shield, the quantity ΔT increases in the interval $\Delta T \in (0.1845, 0.6103)$.

The linear drainage model adopted in the present study was proposed by Joukowski [10] for the calculation of groundwater inflow to irrigation ditches and rivers; later, it was used by Numerov and some other researches. In formulating boundary-value problems describing filtration to linear sinks, it is natural to specify the pressure head on them. Another schematization of horizontal drains by means of point sinks [5] corresponds to tubular drains and water intakes and includes specification of their filtration discharge in the original formulation. Meanwhile, in hydromeliorative practice, one usually has to specify the pressure head on the drain, whose allowance in the boundary-value problem requires additional calculations.

For drains of small width, which are completely flooded even in the case of insignificant infiltration, is possible to establish the relationship between the width $2l$ of a linear drain and the diameter δ of a tubular drain for which the filtration discharges Q are identical for the same values of pressure head on the drains, where $h = 0$, and the outer boundaries of the flows. From the expressions for the complex potentials of the flows produced by single point

and linear sinks for $l = \delta$, it follows that the difference μ between the values of the pressure head h in the patterns compared decreases with distance from the drains to values of about $\delta \exp(-\pi h/Q)$ with increasing pressure heads. Since the intervals of such increase are limited within the limits of the flow region, the quantity μ depends greatly on the drain dimensions. Summarizing the aforesaid, we conclude that a tubular drain of small diameter δ is equivalent to a linear drain of width 2δ. Aver'yanov (see [9]) came to the same conclusion in considering a different flow pattern with a drain.

In numerical calculations, we use the flow pattern to a linear drain, setting $\varepsilon = 0.1$, $\rho = 0.01$, $T_0 = 1.25$, and $h_M = 0$. For each value of the quantity l, which is varied in the range $l \in (10^{-5}, 10^{-2})$, the average ordinate H_0 of the points of the depression curve is calculated. The value obtained is specified, together with the remaining above-listed input parameters, in the subsequent calculation of the characteristics of the flow to a point sink (see [3]); one of them is the diameter δ of the tubular drain on whose contour the pressure $p = 0$ is the same as that on the linear drain. Near the lower boundary of the indicated range of l, the equality $l \approx \delta$ is valid with an error comparable to the calculation error; in the patterns compared, all geometrical parameters of the freshwater fringe also almost coincide. With increasing l, this error increases, and for $l = 0.01$, we have $\delta = 0.0123$. On the lower and upper boundaries of the chosen range of l, the quantity H_0 takes values of $H_0 = 0.3944$ and 0.1673, respectively. As the dimensions of the drains increase, the concentrated effect of the point sink is manifested in somewhat greater deformation of both free boundaries than that for the equivalent linear drains. Thus, for $l = 0.01$ in the linear and tubular drainage patterns (for values of H_0 and T_0 identical for both patterns), we have $\Delta H = 0.1215$ and 0.1218 and $\Delta T = 0.4497$ and 0.4500, respectively.

Conclusions. The analysis of the flow to horizontal linear drains in a fresh groundwater fringe above saline groundwater completes the studies started in [1]. Based on the direct formulation of the corresponding boundary-value problem, the diversity of its physical content is revealed, the effect of each determining parameter on the flow pattern is evaluated, and the relationship between the linear and point drainage models is found. Among the flow features we note the weak dependence of the degree of deformation of the interface and the minimum admissible depth of saline water on the infiltration rate and the pressure head on the drain for its complete flooding and the negligibly small effect of the density of saline water on the position of the depression curve. The latter circumstance allows the calculation results for the flow characteristics at the top of the fresh groundwater fringe to be extended to the filtration model in ground with a confining layer without transforming the calculation formulas. In the boundary-value problem considered, this model can be approached by achieving almost complete flattening of the interface boundary by increasing the parameter ρ.

REFERENCES

1. Yu. I. Kapranov, "Freshwater lens formed by uniform infiltration," *Prikl. Mat. Mekh.*, **38**, No. 6, 1048–1055 (1974).
2. P. Ya. Polubarinova-Kochina, *Theory of Groundwater Motion* [in Russian], Nauka, Moscow (1977).
3. Yu. I. Kapranov and V. N. Émikh, "Boundary-value problem of drainage in a fresh groundwater fringe above saline groundwater," *J. Appl. Mech. Tech. Phys.*, **45**, No. 5, 679–691 (2004).
4. P. F. Byrd and M. D. Friedman, *Handbook of Elliptic Integrals for Engineers and Scientists*, Springer, Berlin (1971).
5. V. V. Vedernikov, *Theory of Filtration and Its Applications in Irrigation and Drainage* [in Russian], Gosstroizdat, Moscow–Leningrad (1939).
6. B. M. Degtyarev and V. A. Kalantaev, *Vacuum Drainage on Irrigated Land* [in Russian], Kolos, Moscow (1978).
7. V. N. Émikh, "Boundary-value problem of a drained freshwater fringe and its applications," *Prikl. Mat. Mekh.*, **60**, No. 3, 494–503 (1996).
8. P. Ya. Polubarinova-Kochina, "On a fresh-water lens above saline water," *Prikl. Mat. Mekh.*, **20**, No. 3, 418–420 (1956).
9. S. F. Aver'yanov, "Salinating effect of filtration from channels," in: *Effect of Irrigation on Groundwater Regime* [in Russian], Izd. Akad. Nauk SSSR, Moscow (1959), pp. 44–130.
10. N. E. Joukowski, "Water percolation through dams," in: *Collected Papers* [in Russian], Vol. 7, Gostekhteoretizdat, Moscow (1950) pp. 297–332.